

CHAPTER 2

CONSTITUTIVE EQUATION OF PIEZOELECTRIC CURVILINEAR MOTORS

A piezoelectric laminated curvilinear arc can serve as a stator of the curvilinear motor to drive the rotor along its alignment. The objective of this chapter is to establish the constitutive equations of the piezoelectric curvilinear stator. The mathematical model and governing equations of curvilinear arcs bonded with piezoelectric actuator patches are derived. The piezoelectric actuation force is also presented. Analysis of these equations is crucial for determination of traveling wave in the curvilinear stator.

2.1. BACKGROUND

Piezoelectric ultrasonic motors have been continuously developed and commercially used in many applications, such as micro-positioners, camera lenses control, actuators for miniaturized devices and small robots [1-4]. One major advantage of the piezoelectric motors over the conventional motors is the high power to weight ratio [2-4]. There are many types of piezoelectric motors classified by their movements, e.g., 1) linear motors [5-7] and 2) rotary motors [8]. In addition to these, a "curvilinear motor" is a relatively new type of piezoelectric motors [9], which provides curvilinear motions for the rotors. This new device can be applied to robot joints, wrist motors, orientated tables, curvilinear drive mechanisms, micro positioning, curvilinear conveyers and movable structures, etc.

The fundamental principle of the traveling wave ultrasonic motors is based on the traveling waves generated on the stator driving the rotor [2-4,8]. Traveling waves of ultrasonic rotary motors are generated by piezoelectric actuators bonded on a circular disk or ring with assumed free boundary conditions. Both analytical and finite element (FE) methods have been used to study vibration characteristics of rotary ultrasonic motors [10-12]. On the other hand, there are piezoelectric ultrasonic motors made of finite-length stators, such as ultrasonic linear [7] and curvilinear motors [9], in which their stator structures are made of either a beam or a circular arc, respectively. Analytical mode shapes of the arc structure with fully laminated actuator have been reported [9]. Traveling waves of the linear or curvilinear ultrasonic motors have also been studied by using the FE method [7,13,14]. However, these linear and curvilinear ultrasonic motors are fully laminated with piezoelectric actuators. Actuation force and moment of the piezoelectric patch have been analyzed and results show that the control force and moment depend on many parameters such as actuator size, location and thickness [9]. Boundary condition of the finite-length media usually reflects the traveling wave when the wave reaches the boundaries. This causes undesirable interfering standing waves [14]. Moreover, there are several

parameters that have effects on characteristics of the traveling wave of the finite length media, e.g., actuator size, operating frequency, actuator location and actuator pattern [9]. The governing equations of fully laminated piezoelectric curvilinear arc motor have been reported [14], in which the system structural stiffness is distributed evenly. The effect of damping materials at the supports of the piezoelectric arc structure has also been studied [14]. Results show that the damping effect causes the wave amplitude decreased because it absorbs vibration energy. Later, the experimental study of piezoelectric curvilinear arc stator has been carried out [15]. Design, fabrication and testing of the piezoelectric arc stator have been presented, and experimental results were compared well with the FE results. The research methodology is used again in this work to study the partially laminated piezoelectric arc stator.

In practical applications, partially bounded actuators can reduce weight, material cost, power consumption and easier maintenance of ultrasonic motors. However, specific location and pattern of piezoelectric actuators on the arc structure have not been thoroughly investigated. Based on established design procedures and mathematical model [14,15], the partially laminated actuator pattern on the curvilinear structure is firstly introduced in this study. Even though the general governing equations are similar to those presented before [14], because they are all curvilinear arc structures, but the number and location of partially laminated piezoelectric actuators are totally different, hence, yielding different system response and more effective motors. Dynamic characteristics of the arc stator partially bonded with piezoelectric actuators are analyzed first. Then, governing equations of the curvilinear arc stator are presented.

2.2. DYNAMICS OF A CURVILINEAR ARC STATOR

A curvilinear arc stator driving a rotor is illustrated in Figure 2.1. Its dynamic characteristics and vibration behavior will be analyzed in this section. The curvilinear arc stator drives and guides a rotor along the curvilinear arc to any specific angular position on the arc surface. Figure 2.1 also illustrates the arc spatial coordinate system defined as $\alpha_1 = \phi$, $\alpha_2 = y$ and $\alpha_3 = z$. The Lamé parameters corresponding to the arc coordinates are $A_1 = R$ and $A_2 = 1$ and the radii of curvature are $R_1 = R$ and $R_2 = \infty$. It is assumed that mass of the piezoelectric patch has no influence to the arc dynamics in order to simplify the system governing equations.

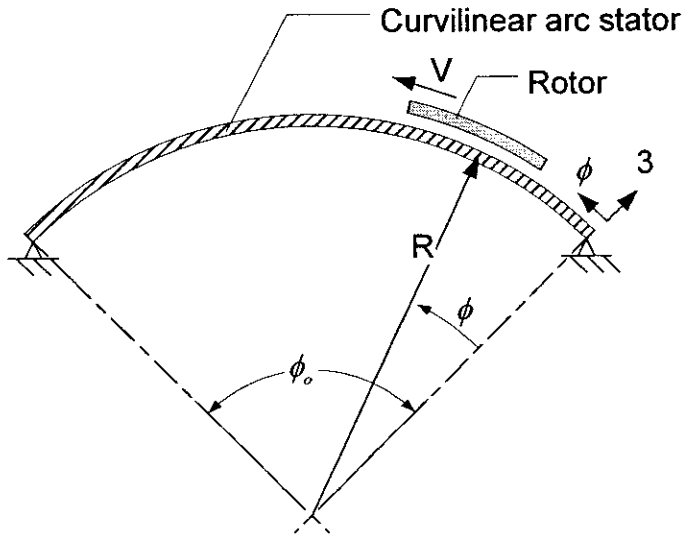


Figure 2.1. Schematic diagram of the curvilinear arc motor.

A curvilinear arc is assumed slender [16], i.e., the ratio of thickness to length is very small. Thus, the thin shell theory can be applied to define the system equations. Assume that there are no deflections in the y -direction (depth direction) and changes with respect to the y -direction can be neglected. Hence there are two equations of motion respectively in the ϕ - and 3-directions describing the dynamic response, Figure 2.2.

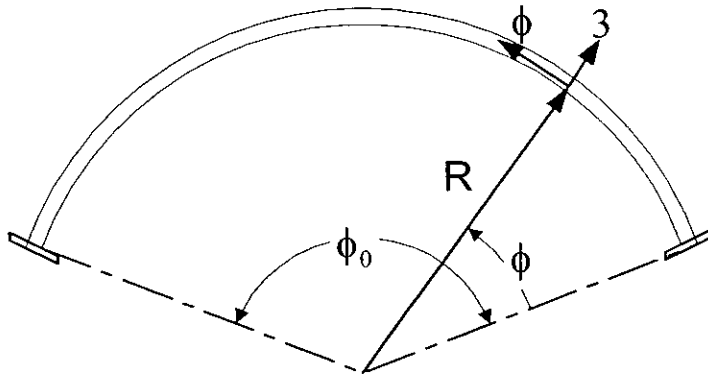


Figure 2.2. Coordinate system of a curvilinear arc.

Substituting the Lamé parameters and radii of curvature into the system equations of a generic double-curvature thin shell and simplifying the equations yields the equations of motion of the arc stator respectively in the ϕ - and 3-directions. There are

$$-\frac{\partial N_{\phi\phi}}{\partial\phi} - Q_{\phi 3} + R\rho h \frac{\partial^2 u_{\phi}}{\partial t^2} = Rq_{\phi}, \quad (2.1)$$

$$-\frac{\partial Q_{\phi 3}}{\partial \phi} + N_{\phi\phi} + R\rho h \frac{\partial^2 u_3}{\partial t^2} = Rq_3; \quad (2.2)$$

and

$$Q_{\phi 3} = \frac{1}{R} \frac{\partial M_{\phi\phi}}{\partial \phi}; \quad (2.3)$$

where $N_{\phi\phi}$ is the membrane force; $M_{\phi\phi}$ is the bending moment; $Q_{\phi 3}$ denotes the traverse shear stress resultant; R is the arc radius; q_i is the external excitation; ρ is the mass density; h is the shell thickness, and u_i is the displacement in the i -direction. Note that q_i can also be discrete or distributed control forces. Membrane force $N_{\phi\phi}$ and bending moment $M_{\phi\phi}$ are functions of membrane strains s_{ij}° and bending strains k_{ij} defined as

$$N_{\phi\phi} = K(s_{\phi\phi}^{\circ} + \mu s_{\gamma\gamma}^{\circ}), \quad (2.4)$$

$$M_{\phi\phi} = D(k_{\phi\phi} + \mu k_{\gamma\gamma}), \quad (2.5)$$

where $K = (\gamma h)/(1 - \mu^2)$ is the membrane stiffness; $D = (\gamma h^3)/[12(1 - \mu^2)]$ is the bending stiffness; γ is Young's modulus; and μ is Poisson's ratio. The strain-displacement relations of the thin arc stator are

$$s_{\gamma\gamma}^{\circ} = 0, \quad (2.6)$$

$$s_{\phi\phi}^{\circ} = \frac{1}{R} \left(\frac{\partial u_{\phi}}{\partial \phi} + \frac{u_3}{R} \right); \quad (2.7)$$

$$k_{\gamma\gamma} = 0, \quad (2.8)$$

$$k_{\phi\phi} = \frac{1}{R} \frac{\partial \beta_{\phi}}{\partial \phi}; \quad (2.9)$$

and the rotation angle is $\beta_{\phi} = \frac{1}{R} \left(u_{\phi} - \frac{\partial u_3}{\partial \phi} \right)$. Substituting Eqs.(2.3-9) into Eqs.(2.1) and (2.2)

yields the equations of motion in the ϕ - and 3-directions respectively as

$$\frac{D}{R^4} \left(\frac{\partial^2 u_{\phi}}{\partial \phi^2} - \frac{\partial^3 u_3}{\partial \phi^3} \right) + \frac{K}{R^2} \left(\frac{\partial^2 u_{\phi}}{\partial \phi^2} + \frac{\partial u_3}{\partial \phi} \right) + q_{\phi} = \rho h \frac{\partial^2 u_{\phi}}{\partial t^2}, \quad (2.10)$$

$$\frac{D}{R^4} \left(\frac{\partial^3 u_{\phi}}{\partial \phi^3} - \frac{\partial^4 u_3}{\partial \phi^4} \right) - \frac{K}{R^2} \left(\frac{\partial u_{\phi}}{\partial \phi} + u_3 \right) + q_3 = \rho h \frac{\partial^2 u_3}{\partial t^2}. \quad (2.11)$$

Note that although the arc dynamic equations are defined with respect to a unit width, the width effect to the stiffness and mass are considered in the frequency calculation presented next. Even and odd flexural mode shapes U_{ij} and natural frequencies f_k of a curvilinear arc with simply supported boundary conditions are defined as follows [16,19]

$$f_k = \frac{k^2 \pi^2}{2\pi(R\phi_0)^2} \left[\frac{\{1 - (\frac{\phi_0}{k\pi})^2\}^2}{1 + 3(\frac{\phi_0}{k\pi})^2} \right]^{1/2} \sqrt{\frac{YI}{\rho hb}}; \text{ for } k=2,4,6,\dots \quad (2.12)$$

$$U_{\phi_k} = \frac{\phi_0}{k\pi} \left[1 - \cos\left(\frac{k\pi\phi}{\phi_0}\right) \right]; \text{ for } k=2,4,6,\dots \quad (2.13)$$

$$U_{3k} = -\sin\left(\frac{k\pi\phi}{\phi_0}\right); \text{ for } k=2,4,6,\dots \quad (2.14)$$

and

$$f_k = \frac{k^2 \pi^2}{2\pi(R\phi_0)^2} \left[\frac{\{1 - (\frac{\phi_0}{k\pi})^2\}^2}{1 + \frac{1}{k^2} + 2(\frac{\phi_0}{k\pi})^2} \right]^{1/2} \sqrt{\frac{YI}{\rho hb}}; \text{ for } k=3,5,7,\dots \quad (2.15)$$

$$U_{\phi_k} = -\frac{\phi_0}{k\pi} \left[\cos\left(\frac{k\pi\phi}{\phi_0}\right) - \frac{1}{\pi^3} \cos\left(\frac{\pi\phi}{\phi_0}\right) \right]; \text{ for } k=3,5,7,\dots \quad (2.16)$$

$$U_{3k} = -\sin\left(\frac{k\pi\phi}{\phi_0}\right) + \frac{1}{k} \sin\left(\frac{\pi\phi}{\phi_0}\right); \text{ for } k=3,5,7,\dots \quad (2.17)$$

where k is the mode number; f_k is the natural frequency in (Hz); Y is the modulus of elasticity; I is the cross-section area moments of inertia; ρ is the mass density; h is the thickness of the arc; b is the width of the arc; U_{ϕ_k} , U_{3k} are the k^{th} flexural mode shapes corresponding to the ϕ - and 3-direction; ϕ is the angular position of the arc; ϕ_0 is opening angle of the arc.

2.3. PIEZOELECTRIC ACTUATION FORCES AND MOMENTS ON A CURVILINEAR ARC STATOR

A piezoelectric patch bonded on the curvilinear arc stator introduces actuation forces and moments resulting in curvilinear driving actions. The effect of actuation force $N_{\phi\phi}^c$ and moment $M_{\phi\phi}^c$ induced by the piezoelectric actuator patch can be added to the dynamic equations of the curvilinear arc, Eqs.(2.1) and (2.2), and presented as

$$\frac{\partial(N_{\phi\phi} - N_{\phi\phi}^c)}{\partial\phi} + Q_{\phi_3} + Rq_{\phi} = R\rho h \frac{\partial^2 u_{\phi}}{\partial t^2}, \quad (2.18)$$

$$\frac{\partial Q_{\phi_3}}{\partial\phi} - (N_{\phi\phi} - N_{\phi\phi}^c) + Rq_3 = R\rho h \frac{\partial^2 u_3}{\partial t^2}; \quad (2.19)$$

and

$$Q_{\phi_3} = \frac{1}{R} \frac{\partial(M_{\phi\phi} - M_{\phi\phi}^c)}{\partial\phi}. \quad (2.20)$$

Forced response of the arc system can be determined by the modal participation method. It is assumed that the excitation force is independent of the shell motion and that the amount of participation of each mode in the total dynamic response is defined by the modal participation factor [17]. Thus, the total response of the arc $u_i(\phi, t)$ can be written as

$$u_i(\phi, t) = \sum_{k=2}^{\infty} \eta_k(t) U_k(\phi), \text{ for } i = \phi, 3, \quad (2.21)$$

where $\eta_k(t)$ is the modal participation factor and $U_k(\phi)$ is the mode shape function in the i -direction. Using Eq.(2.21) and imposing modal orthogonality, one can derive the modal equation of the curvilinear arc as

$$\ddot{\eta}_k + 2\zeta_k \omega_k \dot{\eta}_k + \omega_k^2 \eta_k = \hat{F}_k^m(t) + \hat{F}_k^c(t) \equiv \hat{F}_k(t), \quad (2.22)$$

where the modal damping ratio $\zeta_k = c/(2\rho h\omega_k)$ and c is the damping factor usually experimentally estimated; ω_k is the k^{th} mode natural frequency; $\hat{F}_k^m(t)$ is the mechanical excitation; $\hat{F}_k^c(t)$ is the electrical control excitation; $\hat{F}_k(t)$ is the total modal control force. In this case, it is assumed that the mechanical excitation is neglected, thus the excitation force is only the electrical control excitation. Then the modal control force $\hat{F}_k(t)$ becomes

$$\hat{F}_k(t) = \frac{1}{\rho h N_k} \iint_{y, \phi} \left\{ \sum_i L_i^c(\phi^a) U_k \right\} A_1 A_2 d\phi dy, \text{ for } i = \phi, 3, \quad (2.23)$$

where $N_k = \iint_{y, \phi} \left\{ \sum_i U_k^2 \right\} A_1 A_2 d\phi dy$; $L_i^c(\phi^a)$ is a Love's operator derived from the converse piezoelectric effect and it is assumed that only a transverse voltage ϕ^a is considered [18]. Also, note that $L_i^c(\phi^a)$ is a function of the spatial coordinate and time. Thus,

$$L_\phi^c(\phi^a) = -\frac{1}{R} \left(\frac{\partial N_{\phi\phi}^c}{\partial \phi} + \frac{1}{R} \frac{\partial M_{\phi\phi}^c}{\partial \phi} \right), \quad (2.24)$$

$$L_3^c(\phi^a) = -\frac{1}{R} \left(\frac{1}{R} \frac{\partial^2 M_{\phi\phi}^c}{\partial \phi^2} - N_{\phi\phi}^c \right). \quad (2.25)$$

2.3.1. Actuation Forces and Moments

The curvilinear arc stator is bonded with a piezoelectric actuator patch defined from ϕ_1 to ϕ_2 in the angular position and has the same width as the arc stator b as illustrated in Figure 2.3. It is assumed that the radius of curvature of the actuator patch is $(R + h/2 + h^a/2) \approx R$ where h is the stator thickness and h^a is the actuator thickness. Thus, the effective actuator area S^e can be approximated as $Rb(\phi_2 - \phi_1)$.

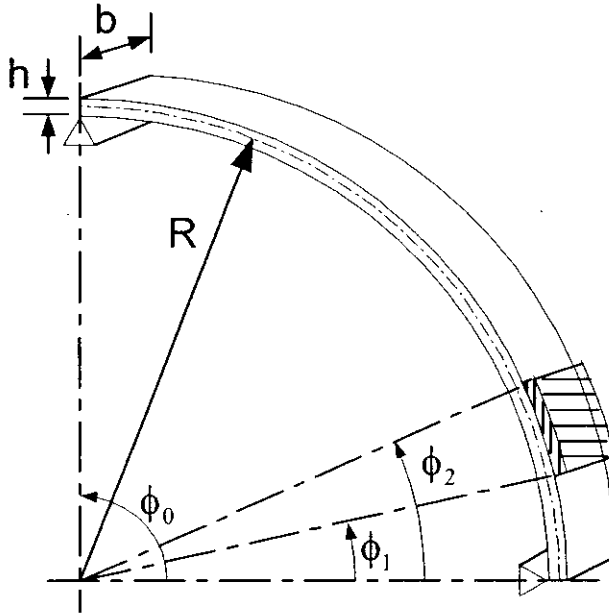


Figure 2.3. A piezoelectric laminated curvilinear arc.

It is assumed that only a transverse voltage ϕ^a is applied. If the electrode resistance is neglected, the voltage on the piezoelectric actuator patch is constant. Thus, an actuator voltage $\phi^a(y, \phi, t)$ applied to the distributed piezoelectric actuator patch is

$$\phi^a(y, \phi, t) = \phi^a(t) [u_s(y - y_1) - u_s(y - y_2)] [u_s(\phi - \phi_1) - u_s(\phi - \phi_2)], \quad (2.26)$$

where u_s represents a unit step function, $u_s(\phi - \phi_i) = 1$ when $\phi \geq \phi_i$, and $= 0$ when $\phi < \phi_i$. The spatial derivatives are

$$\frac{\partial}{\partial \phi} \phi^*(y, \phi, t) = \phi^*(t) [u_s(y - y_1) - u_s(y - y_2)] [\delta(\phi - \phi_1) - \delta(\phi - \phi_2)], \quad (2.27)$$

where $\delta(\cdot)$ is the Dirac delta function: $\delta(\phi - \phi_i) = 1$ when $\phi = \phi_i$, and $= 0$ when $\phi \neq \phi_i$. Then, the actuation force $N_{\phi\phi}^c$ and a actuation moment $M_{\phi\phi}^c$ in the ϕ -direction induced by the piezoelectric actuator patch can be defined as

$$N_{\phi\phi}^c = Y_p d_{31} \phi^* [u_s(y - y_1) - u_s(y - y_2)] [u_s(\phi - \phi_1) - u_s(\phi - \phi_2)], \quad (2.28)$$

$$M_{\phi\phi}^c = r^* Y_p d_{31} \phi^* [u_s(y - y_1) - u_s(y - y_2)] [u_s(\phi - \phi_1) - u_s(\phi - \phi_2)], \quad (2.29)$$

where Y_p is the actuator elastic modulus; d_{31} is the piezoelectric strain constant; r^* is the effective moment arm (distance from the neutral surface to the mid-plane of the actuator patch).

2.3.2. Micro-actuation Force Components of Piezoelectric Actuator Patches

An actuation force induced by a segmented piezoelectric patch defined from ϕ_1 to ϕ_2 in the ϕ -direction and from y_1 to y_2 in the y -direction is evaluated and its microscopic membrane/bending characteristics are analyzed. Expanding the modal actuation force, Eq. (2.23), yields

$$\hat{F}_k = \frac{1}{\rho h N_{x,y,\phi}} \iint \{L_{\phi}^c(\phi_3) U_{\phi k} + L_{3k}^c(\phi_3) U_{3k}\} A_1 A_2 d\phi dy. \quad (2.30)$$

Substituting Love's operators, Eqs.(2.24) and (2.25), into the modal force gives

$$\begin{aligned} \hat{F}_k = & \frac{1}{\rho h N_{x,y,\phi}} \iint \left\{ \left(-\frac{1}{R} \left(\frac{\partial N_{\phi\phi}^c}{\partial \phi} + \frac{1}{R} \frac{\partial M_{\phi\phi}^c}{\partial \phi} \right) \right) U_{\phi k} \right. \\ & \left. + \left(-\frac{1}{R} \left(\frac{1}{R} \frac{\partial^2 M_{\phi\phi}^c}{\partial \phi^2} - N_{\phi\phi}^c \right) \right) U_{3k} \right\} A_1 A_2 d\phi dy \end{aligned} \quad (2.31)$$

The above equation, Eq. (2.31), implies that the modal actuation force consists of four actuation force/moment actions. There are 1) the membrane component $\hat{T}_{k-U\phi,mem}$ induced by $U_{\phi k}$, 2) the bending component $\hat{T}_{k-U\phi,bend}$ induced by $U_{\phi k}$, 3) the membrane component $\hat{T}_{k-U_3,mem}$ induced by U_{3k} , and 4) the bending component $\hat{T}_{k-U_3,bend}$ induced by U_{3k} . Detailed derivations of the actuation force components are respectively defined next.

2.3.2.1. Membrane Actuation Force Components

The membrane actuation force component $\hat{T}_{k_U\phi,mem}$ induced by $U_{\phi k}$ can be described as

$$\hat{T}_{k_U\phi,mem} = \frac{1}{\rho h N_k} \int \int_{y_1}^{y_2} \left\{ \left(-\frac{1}{R} \frac{\partial N_{\phi\phi}^c}{\partial \phi} \right) U_{\phi k} \right\} A_1 A_2 d\phi dy. \quad (2.32)$$

Substituting Eqs.(2.26-28) into Eq.(2.32) gives

$$\begin{aligned} \hat{T}_{k_U\phi,mem} &= -\frac{Y_p d_{31} \phi^a}{\rho h N_k} \int_0^{\phi_2} \int_{y_1}^{y_2} \{ ([u_s(y-y_1) - u_s(y-y_2)]) [\delta(\phi-\phi_1) - \delta(\phi-\phi_2)] U_{\phi k} \} dy d\phi \\ &= -\frac{Y_p d_{31} \phi^a}{\rho h N_k} \int_0^{\phi_2} [\delta(\phi-\phi_1) - \delta(\phi-\phi_2)] U_{\phi k} \int_{y_1}^{y_2} ([u_s(y-y_1) - u_s(y-y_2)]) dy d\phi \\ &= -\frac{Y_p d_{31} \phi^a}{\rho h N_k} (y_2 - y_1) \int_0^{\phi_2} [\delta(\phi-\phi_1) - \delta(\phi-\phi_2)] U_{\phi k} d\phi. \end{aligned}$$

Thus,

$$\hat{T}_{k_U\phi,mem} = \frac{Y_p d_{31} \phi^a}{\rho h N_k} (y_2 - y_1) (U_{\phi k} \Big|_{\phi=\phi_2} - U_{\phi k} \Big|_{\phi=\phi_1}). \quad (2.33)$$

Assume that the piezoelectric actuator patch has the same width as the arc stator, i.e., $y_2 - y_1 = b$ and also define $U_{\phi k} \Big|_{\phi=\phi_i} = U_{\phi_i k}$. The membrane actuation force component induced by $U_{\phi k}$ of an actuator patch $[\phi_1, \phi_2]$ can be rewritten as

$$\hat{T}_{k_U\phi,mem} = \frac{Y_p d_{31} \phi^a b}{\rho h N_k} (U_{\phi_2 k} - U_{\phi_1 k}). \quad (2.34)$$

Following the same procedures, one can derive the membrane actuation force component

$\hat{T}_{k_U_3,mem}$ induced by U_{3k} as follows

$$\hat{T}_{k_U_3,mem} = \frac{Y_p d_{31} \phi^a b}{\rho h N_k} (U_{\phi_2 k} - U_{\phi_1 k}). \quad (2.35)$$

Substituting Eqs.(2.26-28), Eq.(2.35) yields

$$\begin{aligned}
\hat{T}_{k-U_3,mem} &= \frac{Y_p d_{31} \phi^a}{\rho h N_k} \int_y \int_{\phi} \{ [u_s(y-y_1) - u_s(y-y_2)] [u_s(\phi-\phi_1) - u_s(\phi-\phi_2)] U_{3k} \} d\phi dy \\
&= \frac{Y_p d_{31} \phi^a}{\rho h N_k} \int_0^{\phi_2} [u_s(\phi-\phi_1) - u_s(\phi-\phi_2)] U_{3k} \int_{y_1}^{y_2} [u_s(y-y_1) - u_s(y-y_2)] dy d\phi \\
&= \frac{Y_p d_{31} \phi^a}{\rho h N_k} (y_2 - y_1) \int_0^{\phi_2} [u_s(\phi-\phi_1) - u_s(\phi-\phi_2)] U_{3k} d\phi.
\end{aligned}$$

Hence,

$$\hat{T}_{k-U_3,mem} = \frac{Y_p d_{31} \phi^a}{\rho h N_k} (y_2 - y_1) \int_{\phi_1}^{\phi_2} U_{3k} d\phi. \quad (2.35b)$$

Thus, the membrane actuation component induced by U_{3k} of an actuator patch $[\phi_1, \phi_2]$ becomes

$$\hat{T}_{k-U_3,mem} = \frac{Y_p d_{31} \phi^a b}{\rho h N_k} \int_{\phi_1}^{\phi_2} U_{3k} d\phi. \quad (2.36)$$

2.3.2.2. Bending Actuation Components

The bending actuation component $\hat{T}_{k-U\phi,bend}$ induced by $U_{\phi k}$ can be described as

$$\hat{T}_{k-U\phi,bend} = \frac{1}{\rho h N_k} \int_y \int_{\phi} \left\{ \left(-\frac{1}{R^2} \frac{\partial M_{\phi\phi}^c}{\partial \phi} \right) U_{\phi k} \right\} A_1 A_2 d\phi dy. \quad (2.37)$$

Substituting Eqs.(2.26), (2.27) and (2.29) into Eq.(2.37) yields

$$\begin{aligned}
\hat{T}_{k-U\phi,bend} &= -\frac{1}{R \rho h N_k} \int_y \int_{\phi} \left\{ \frac{\partial M_{\phi\phi}^c}{\partial \phi} U_{\phi k} \right\} d\phi dy \\
&= -\frac{r^a Y_p d_{31} \phi^a}{R \rho h N_k} \int_0^{\phi_2} [\delta(\phi-\phi_1) - \delta(\phi-\phi_2)] U_{\phi k} \int_{y_1}^{y_2} [u_s(y-y_1) - u_s(y-y_2)] dy d\phi \\
&= -\frac{r^a Y_p d_{31} \phi^a}{R \rho h N_k} (y_2 - y_1) \int_0^{\phi_2} [\delta(\phi-\phi_1) - \delta(\phi-\phi_2)] U_{\phi k} d\phi \\
&= \frac{r^a Y_p d_{31} \phi^a}{R \rho h N_k} (y_2 - y_1) (U_{\phi k} \Big|_{\phi=\phi_2} - U_{\phi k} \Big|_{\phi=\phi_1}).
\end{aligned} \quad (2.37b)$$

Thus, the bending actuation component induced by $U_{\phi k}$ can be expressed as

$$\hat{T}_{k_{-U\phi},bend} = \frac{r^{\circ}Y_p d_{31} \phi^{\circ} b}{R\rho h N_k} (U_{\phi_2,k} - U_{\phi_1,k}). \quad (2.38)$$

Furthermore, one can follow the same procedures and determine the bending actuation component $\hat{T}_{k_{-U_3},bend}$ induced by U_{3k} as follows:

$$\hat{T}_{k_{-U_3},bend} = \frac{1}{\rho h N_k} \int \int \left\{ -\frac{1}{R^2} \frac{\partial^2 M_{\phi\phi}^c}{\partial \phi^2} U_{3k} \right\} A_1 A_2 d\phi dy; \quad (2.39)$$

Substituting Eqs.(2.26), (2.27) and (2.29) into Eq.(2.39) gives

$$\begin{aligned} \hat{T}_{k_{-U_3},bend} &= -\frac{1}{\rho h N_k} \int \int \frac{1}{R} \frac{\partial^2 M_{\phi\phi}^c}{\partial \phi^2} U_{3k} d\phi dy \\ &= -\frac{r^{\circ}Y_p d_{31} \phi^{\circ}}{R\rho h N_k} \int_0^{\phi_2} \int_{y_1}^{\phi_2} \frac{\partial^2}{\partial \phi^2} \{ [u_s(y-y_1) - u_s(y-y_2)] [u_s(\phi-\phi_1) - u_s(\phi-\phi_2)] \} \\ &\quad \cdot U_{3k} dy d\phi \\ &= -\frac{r^{\circ}Y_p d_{31} \phi^{\circ}}{R\rho h N_k} \int_0^{\phi_2} \int_{y_1}^{\phi_2} \frac{\partial}{\partial \phi} \{ [u_s(y-y_1) - u_s(y-y_2)] [\delta(\phi-\phi_1) - \delta(\phi-\phi_2)] \} \\ &\quad \cdot U_{3k} dy d\phi \\ &= -\frac{r^{\circ}Y_p d_{31} \phi^{\circ}}{R\rho h N_k} \int_0^{\phi_2} \frac{\partial}{\partial \phi} \{ \delta(\phi-\phi_1) - \delta(\phi-\phi_2) \} U_{3k} \int_{y_1}^{y_2} [u_s(y-y_1) - u_s(y-y_2)] \\ &\quad \cdot dy d\phi \\ &= -\frac{r^{\circ}Y_p d_{31} \phi^{\circ}}{R\rho h N_k} (y_2 - y_1) \int_0^{\phi_2} \frac{\partial}{\partial \phi} \{ \delta(\phi-\phi_1) - \delta(\phi-\phi_2) \} U_{3k} d\phi; \end{aligned}$$

Applying the integration by part, one get

$$\begin{aligned}
\hat{T}_{k-U_3, \text{bend}} &= -\frac{r^a Y_p d_{31} \phi^a}{R \rho h N_k} (y_2 - y_1) \int_0^{\phi_0} U_{3k} \frac{\partial}{\partial \phi} \{ \delta(\phi - \phi_1) - \delta(\phi - \phi_2) \} d\phi \\
&= -\frac{r^a Y_p d_{31} \phi^a}{R \rho h N_k} (y_2 - y_1) \\
&\quad \cdot [U_{3k} \{ \delta(\phi - \phi_1) - \delta(\phi - \phi_2) \}] \Big|_0^{\phi_0} - \int_0^{\phi_0} \{ \delta(\phi - \phi_1) - \delta(\phi - \phi_2) \} \frac{\partial U_{3k}}{\partial \phi} d\phi \\
&= \frac{r^a Y_p d_{31} \phi^a}{R \rho h N_k} (y_2 - y_1) \left(\frac{\partial U_{3k}}{\partial \phi} \Big|_{\phi=\phi_1} - \frac{\partial U_{3k}}{\partial \phi} \Big|_{\phi=\phi_2} \right).
\end{aligned} \tag{2.39b}$$

Consequently, the bending actuation component induced by U_{3k} can be expressed as

$$\hat{T}_{k-U_3, \text{bend}} = \frac{r^a Y_p d_{31} \phi^a b}{R \rho h N_k} \left(\frac{\partial U_{3k}}{\partial \phi} \Big|_{\phi=\phi_1} - \frac{\partial U_{3k}}{\partial \phi} \Big|_{\phi=\phi_2} \right). \tag{2.40}$$

Accordingly, the actuator characteristics and all microscopic membrane and bending actuation actions in the modal force Eq.(2.31) can be expressed as

$$\hat{F}_k = \hat{T}_{k-U\phi, \text{mem}} + \hat{T}_{k-U_3, \text{mem}} + \hat{T}_{k-U\phi, \text{bend}} + \hat{T}_{k-U_3, \text{bend}}. \tag{2.41}$$

The modal actuation force \hat{F}_k and its membrane/bending components $\hat{T}_{k-U_{i,j}}$ depend on actuator locations, modal characteristics, actuator material properties and control voltage. To calculate the actual modal actuation force and membrane/bending components, the material properties need to be evaluated and a **modal actuation factor** (\hat{F}_k / ϕ^a) is defined as the magnitude of the modal force per unit control voltage [(N/kg)/V]. The response of the curvilinear arc depends on the modal actuation force. Various types of piezoelectric actuator patterns yield different outcomes. The governing equations of system presented in this chapter will be used in the mathematical model to determine the actuator patterns that yields traveling wave in the next chapter.